Supplementary Methods

Histochemistry Staining

Immunohistochemistry was performed with VECTASTAIN Elite ABC peroxidase kit following manufacturer's instructions (Vector Laboratories, Burlingame, CA, USA) and counterstained with Novocastra Hematoxylin (Leica, Newcastle upon Tyne, UK). 5 μm sections were stained with CD73 (Sigma-Aldrich, St. Louis, MO, USA), Ki67 (12202, Cell Signaling Technology, Danvers, MA, USA), and cleaved caspase-3 (9579, Cell Signaling Technology, Danvers, MA, USA) antibodies.

The intensity score for immunohistochemistry was calculated by examining the stain intensity (0 = none; 1 = weak; 2 = intermediate, 3 = strong) and the proportion of the percentage of positively stained cell (0 = none; 1 = <5%; 2 = 5–25%; 3 = 26–50%; 4 = 51–75%; 5 = >75%). These scores were multiplied together to generate the final histoscore. Images were captured at 20X.

H&E staining was performed by deparaffinization and hydration through graded xylenes and ethanol before submerging in water. Slides were exposed to Gill hematoxylin stain (Fisher Chemical, Geel, Belgium) for 5 min, rinsed, exposed to acid alcohol (75% ethanol + 1/25000 HCl %v/v), rinsed, and incubated within an ammonia solution (0.084% NH4OH %w/v), before submerging in water for 5 min. Slides were exposed to 80% ethanol before submerging in alcoholic eosin Y 515 (Leica) for 2 min. Slides were then exposed to 95% and 100% ethanol before submerging in xylene for 2 min each. Images were captured at 10X.

Representative images were taken by finding three tissues near the median cohort weight and volume was used to break a tie. In the case of survival, the three tissues near

the median survival were used. Three tissues were examined and the tissue with the median Ki67 was chosen to be the representative tissue.

qRT-PCR

RNA isolation and qRT-PCR was performed as described previously [1], but analyzed on QuantStudio 5 Real-Time PCR System (Thermo Fisher Scientific, Waltham, MA, USA). Primers used for *Nt5e* were 5'-GGACATTTGACCTCGTCCAAT-3' (forward) and 5'-GGGCACTCGACACTTGGTG-3' (reverse), and 5'-GGCTGTATTCCCCTCCATCG-3' (forward) and 5'-CCAGTTGGTAACAATGCCATGT–3' (reverse) for *Actb*.

Immunoblotting

Protein isolation and western blotting were performed as described previously [2], but with nitrocellulose membranes. In short, cells were washed twice with PBS and utilized radio-immunoprecipitation assay for lysis by shaking for 10 min on ice. Lysates were centrifuged at 13000 rpm for 10 min at 4°C to collect the supernatant. Bradford assay was used to determine the protein concentration. An equal amount of protein was loaded in each well for western blotting. Specific proteins were probed by using primary antibodies against CD73 (Cell Signaling Technology) and actin (JLA20; Developmental Studies Hybridoma Bank, IA, USA).

Flow cytometry

Peripheral blood was collected through submandibular bleeding [3] in accordance with IACUC, lysed with ACK buffer (150mM NH4Cl, 10mM KHCO3, 0.1 mM EDTA, pH 7.3), and processed for BD LSRII by staining with LIVE/DEAD Fixable Aqua Dead Cell Stain Kit (Life Technologies Corporation, Eugene, OR, USA). Sample volumes were then split

in half with primary conjugated antibodies CD3ε (100206, PE), CD19 (115520, PE-Cy7), CD8α (100711, APC), CD4 (100414, APC-Cy7), and FoxP3 (126421, AF700) from BioLegend (San Diego, CA, USA) to examine T cell subsets. Myeloid subsets were examined in the second half with Ly6G (127614, APC), Ly6C (128025, APC/Cy7), F4/80 (123120, AF488), Nos2 (696804, AF594) CD11b (101257, BV605), CD11c (117318, PE/CY7) from BioLegend and CD11b (48-0112-82, e450) from Thermo Fisher Scientific and Arg1 (1C5868N, AF700) from R&D Systems. Samples were run on a BD LSR II and analyzed with FlowJo version 10. The pilot study utilized LIVE/DEAD Fixable Aqua Dead Cell Stain, CD3ε (100206, PE), CD8α (100706, FITC), and CD4 (100414, APC-Cy7) from BioLegend.

Mass spectrometry of interstitial fluid

The interstitial fluid was collected as described previously [4, 5]. Briefly, blood was rinsed quickly off tumors before incubating in 250μL saline on ice for 5 min. An additional 250μL saline was given and sporadically mixed by inverting for 10 min. A 5 s spin was performed on a mini-centrifuge before separating tissue from interstitial fluid and freezing in liquid nitrogen. The interstitial fluid was thawed and the supernatant was taken after a spin at 1200 rpm at 4°C for 10 min. Standards were made and processed in parallel with interstitial fluid by taking 200μL of the supernatant or standard and adding 800μL of LC-MS grade methanol on dry ice. Samples were then transferred to a -80°C freezer for 2 h. Samples were spun at 13000 rpm for 10 min and the supernatant was placed in a speedvac until dry. Resuspension was done with LC-MS grade methanol/water/acetonitrile (60:30:10 %vol/vol/vol) and ran through a LC-MS/MS with

standards. Quantification of peak areas were performed using MassLynx (Waters Co., Milford, MA, USA) and normalized with the tumor weight used.

Co-culture assays to examine the effect of MDSCs on T cell activation

$CD4^+$ and $CD8^+$ T cells were harvested from the spleen of healthy immunocompetent C57/B6 mice. MDSCs were harvested from pancreatic tumor-bearing mice using magnetic isolation kit (130-094-538, Miltenyi Biotec, Inc). To determine the effect of MDSCs on T cell activation (cytokine analysis), CFSE-labeled $CD4^+$/$CD8^+$ T cells were co-cultured with or without MDSCs and stimulated *in vitro* for 48 h (Cytokine analysis) with anti-CD3/CD28 Dynabeads (Cat #, 11132D, Thermo Fisher Scientific). For proliferation analysis, the isolated CD4+/CD8+ T cells were pre-stained with CFSE (Cat#, C34554 Thermo Fisher Scientific) and co-cultured in the presence or absence of MDSCs and stimulated in vitro for 96 h with anti-CD3/CD28 Dynabeads and recombinant mouse IL-2 (20ng/mL, Cat # 212-12, PeproTech, Cranbury, NJ). The expression of IFNγ, IL10, and TGFβ and the intensity of CFSE signaling were detected by flow cytometry.

Immunofluorescent imaging CD8 and CD4 cells

Pancreatic tumors were examined for CD4+ and CD8+ T cells using fluorescent immunohistochemistry. Briefly, freshly harvested tumors were embedded in OCT (Cat#, 4583, Sakura Finetek, Torrance, CA), and frozen sections of 6-μm thickness tumor tissues were fixed in 4% paraformaldehyde at room temperature for 10 min. Tumor sections were stained with fluorescent anti-CD4 (Cat #, 100401, BioLegend) or anti-CD8a (Cat #, 100701 BioLegend) overnight at 4°C in a humidified chamber. Subsequently, slides were washed and mounted with ProLong™ Diamond Antifade Mountant with DAPI

(Cat# P36962, Thermo Fisher Scientific). Images were captured with a Zeiss 710 Meta Confocal Laser Scanning Microscope and analyzed using the Zeiss Zen Blue software (Carl Zeiss Microscope, LLC, NY, USA). The CD4+ and CD8+ cells were counted in randomly selected 1.5 m^2 image areas.

Animal cohort sizes and statistics

The luciferase study was performed in female B6(Cg)-Tyrc-2J/J mice implanted with KPC1245 control (n=7), sh*Nt5e*-a (n=10), and sh*Nt5e*-b (n=10). Examining time point differences with KPC1245 began with control (n=15), sh*Nt5e*-a (n=15), and sh*Nt5e*-b (n=14) implanted mice and examined mice at day 20 (n=4 each cohort) and at day 30 using the remaining mice. The presence of metastasis was examined and analyzed using a Fisher's exact test. Animal survival and growth kinetics were performed in female B6(Cg)-*Tyr*$^{c\text{-}2J}$/J mice implanted with control (n=15), sh*Nt5e*-a (n=15), and sh*Nt5e*-b (n=10) KPC1199 cell lines. Male B6(Cg)-*Tyr*$^{c\text{-}2J}$/J mice implanted with control (n=14), sh*Nt5e*-a (n=16), and sh*Nt5e*-b (n=20) KPC1199 were used for tumor burden analysis upon necropsy, cytokine array, and peripheral blood immune profiling. 6-8 week old male Taconic athymic nude mice (CrTac:NCr-Foxn1nu) were implanted with KPC1199 control (n=14), sh*Nt5e*-a (n=10), and sh*Nt5e*-b (n=9) cell lines. C57BL/6NTac male mice were used to model immune depletion, in which KPC1245 control cell-implanted mice were treated with anti-IgG2α/β (n=10), anti-CD4 (n=10), and anti-CD8 (n=9), and KPC1245 sh*Nt5e*-b-implanted mice were treated with anti-IgG2α/β (n=10), anti-CD4 (n=10), and anti-CD8 (n=9). To examine the effects of GM-CSF and MDSCs, cohorts with Sg NT-implanted cells were treated with anti-IgG2β (n=11), GM-CSF (n=10), Sg NT with GM-CSF and anti-Gr-1 (n=11) and knockout cell-implanted mice with IgG2β (n=10), GM-CSF

(n=9), Sg NT with GM-CSF and anti-Gr-1 (n=11). However, one mouse from Sg NT IgG2β was later removed due to a poor implantation and one mouse from Sg NT GM-CSF due to a premature death the night before the necropsy. Combination therapy used saline (n=18), anti-Cd73 antibody (n=20), gemcitabine (n=20), and the combination of the two (n=20) was administered to KPC1245-implanted C57BL/6NTac male mice. Survival for all mice was examined for significance with a Mantel-Cox log-rank test and tumor burden was examined with a one-way ANOVA with Dunnett's multiple comparison test for significance, except when mentioned otherwise. Growth kinetics were examined for significance using a two-way ANOVA with a Bonferroni post-test, except for the knockdown anti-CD4 and anti-CD8 depletion study, as well as anti-CD73 with gemcitabine therapy study. These studies overcame mice deaths using generalized linear mixed model for longitudinal log-normal data incorporating compound symmetry correlation among longitudinal data from the same subjects.

Metastasis scoring

After euthanasia and subsequent necropsy, mice were evaluated for presence of metastasis by gross examination, which visually inspected the spleen, liver, stomach, intestines, lymph, mesentery, peritoneum, and the diaphragm for metastasis.

Statistics and sample sizes

TCGA dataset utilized normal adjacent tissue (n=4) for the mean and standard deviation to examine patients with *NT5E* mRNA expression two Z-scores above (n=19), below (n=0), or within two Z-scores (n=131) of normal adjacent tissue. IQR survival analysis

examined the upper (n=38), lower (n=35), and middle interquartile range (n=73). Differences in quartile sample size is due to first generating quartiles based on mRNA expression before examining if the patient was diagnosed with pancreatic ductal adenocarcinoma with clinical data. ICGC did not have normal samples, and hence a Z-score could not be generated, therefore the upper quartile (n=24) and the lower quartile (n=24) were examined. Both analyses used Mantel-Cox log-rank test for significance. qPCR utilized technical replicates for each group (n=4) and used Kruskal-Wallis test with a Dunn's posttest comparing each knockdown to the control. Peripheral blood flow cytometry consisted of control (n=7), sh*Nt5e*-a (n=8), and sh*Nt5e*-b (n=7) mice and tumor flow cytometry consisted of control (n=10), sh*Nt5e*-a (n=6), and sh*Nt5e*-b (n=9) mice tumors which was compared with a one-way ANOVA with a Dunnett's multiple comparison test. Co-culture was performed without MDSCs (n=5), control with MDSCs (n=5), sh*Nt5e*-a with MDSCs (n=5), and sh*Nt5e*-b with MDSCs (n=5) and analyzed with a one-way ANOVA with a Tukey's multiple comparison test. The tumor cytokine array contained 7 tumors from each group using Dunnett's multiple comparison test for significance.

The ANOVA analyses and Pearson's correlation checked normality assumptions using summary statistics including mean, median, Kurtosis, and Shapiro-Wilk test. A p value of less than 0.05 was considered significant. All error bars represent standard error of mean. All animal experiments were replicated once.

Supplementary references

1 Shukla SK, Dasgupta A, Mehla K, Gunda V, Vernucci E, Souchek J *et al*. Silibinin-mediated metabolic reprogramming attenuates pancreatic cancer-induced cachexia and tumor growth. *Oncotarget* 2015; 6: 41146-41161.

2 Gunda V, Souchek J, Abrego J, Shukla SK, Goode GD, Vernucci E *et al*. MUC1-Mediated Metabolic Alterations Regulate Response to Radiotherapy in Pancreatic Cancer. *Clin Cancer Res* 2017; 23: 5881-5891.

3 Golde WT, Gollobin P, Rodriguez LL. A rapid, simple, and humane method for submandibular bleeding of mice using a lancet. *Lab Anim (NY)* 2005; 34: 39-43.

4 Sullivan MR, Danai LV, Lewis CA, Chan SH, Gui DY, Kunchok T *et al*. Quantification of microenvironmental metabolites in murine cancers reveals determinants of tumor nutrient availability. *Elife* 2019; 8.

5 Haslene-Hox H, Oveland E, Berg KC, Kolmannskog O, Woie K, Salvesen HB *et al*. A new method for isolation of interstitial fluid from human solid tumors applied to proteomic analysis of ovarian carcinoma tissue. *PLoS One* 2011; 6: e19217.

Supplementary Data

Supplementary Figures and Supplementary Figure Legends

Supplementary Figure 1

A Z-score

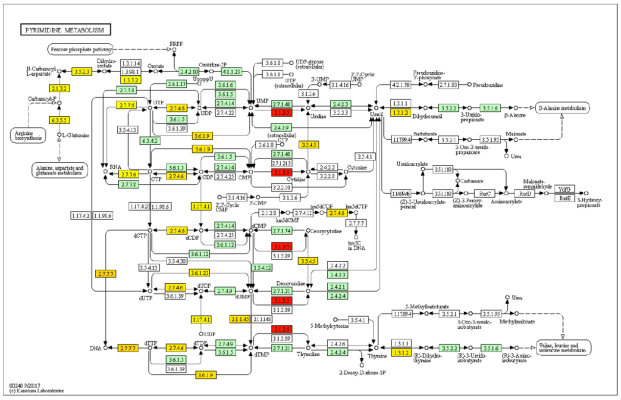

B Z-score

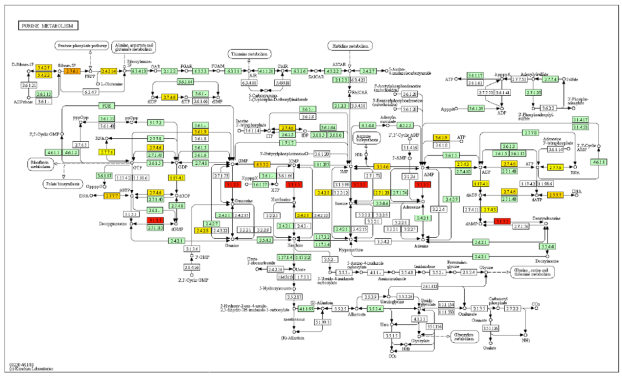

C IQR

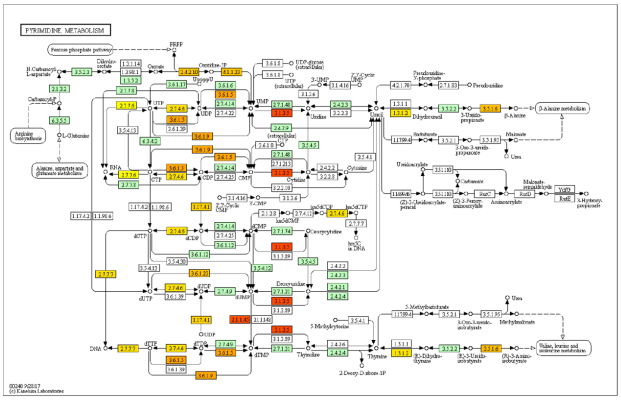

D IQR

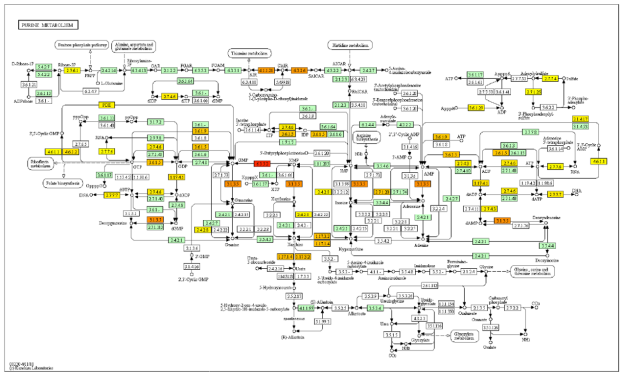

E Z-score

Gene	High vs normal	Low vs normal	High vs Low	All
UROD	3.62E-13	4.80E-03	1.83E-04	2.11E-15
NT5E	7.36E-11	NA	NA	7.36E-11
SGPL1	8.73E-10	9.66E-01	1.57E-01	4.69E-09
ST3GAL6	3.11E-09	3.92E-01	1.08E-04	1.35E-09
GALNT9	2.40E-07	1.19E-02	2.55E-04	2.69E-07
OXSM	2.00E-06	NA	NA	2.00E-06
STT3A	2.91E-06	NA	NA	2.91E-06
PRPS2	3.81E-06	5.87E-01	2.25E-01	1.78E-05
ALG10	5.08E-06	6.89E-01	8.01E-02	2.10E-05
PTGS2	8.28E-06	NA	NA	8.28E-06
NDUFA9	1.36E-05	6.56E-01	5.77E-01	6.76E-05

F IQR

Gene	High vs Normal	Low vs Normal	High vs Low	All
GMPS	7.22E-05	1.04E-01	1.84E-05	8.61E-07
NT5E	7.33E-04	4.25E-01	5.82E-04	1.41E-04
TYMS	1.02E-04	9.59E-01	1.83E-03	1.69E-04
PIP5K1B	5.13E-01	4.23E-05	1.21E-02	1.91E-04
PYGL	2.49E-04	6.94E-01	2.49E-03	2.17E-04
PAICS	3.16E-03	6.64E-02	5.50E-04	2.45E-04
DGKD	9.70E-01	2.23E-04	1.74E-02	6.99E-04
MTHFR	4.89E-01	4.44E-04	2.08E-02	9.97E-04
ATP6V0A1	4.45E-01	8.23E-04	6.70E-03	1.08E-03
EARS2	3.85E-03	3.95E-01	1.26E-03	1.12E-03
POLR3G	2.18E-03	8.09E-01	1.80E-03	1.14E-03

Supplementary Figure 1. Pyrimidine and purine pathways are enriched in the survival-associated enzyme cohorts. A-B Kyoto Encyclopedia of Genes and Genomes' (KEGG) pyrimidine (**A**) and purine (**B**) metabolism pathways were colored according to Mantel-Haenszel log-rank survival p-value of genes when separating cohorts that are two standard deviations away from normal adjacent tissue mRNA (Z-score). **C-D** KEGG's pyrimidine (**C**) and purine (**D**) metabolism pathways colored according to Mantel-Haenszel log-rank survival p-value, however, patients were split into cohorts by the interquartile range (IQR) of a given gene. Genes are colored based on the Mantel-Haenszel log-rank survival p-value < 0.05. Yellow indicates a weaker significant p-value,

orange indicates a moderately significant p-value, and red indicates the top spectrum of the most significant p-value. Green indicates it was not seen as significant, whereas white boxes indicate a non-human gene in the database. The color-coding scale for Z-score and IQR charts are independent of each other. All enzymes within each cohort impact the color scale regardless of their presence within a displayed pathway. **E** Z-score enzyme survival p-values when ranked by high vs. normal mRNA expression. **F** IQR enzyme survival p-values when ranking by all cohorts.

Supplementary Figure 2

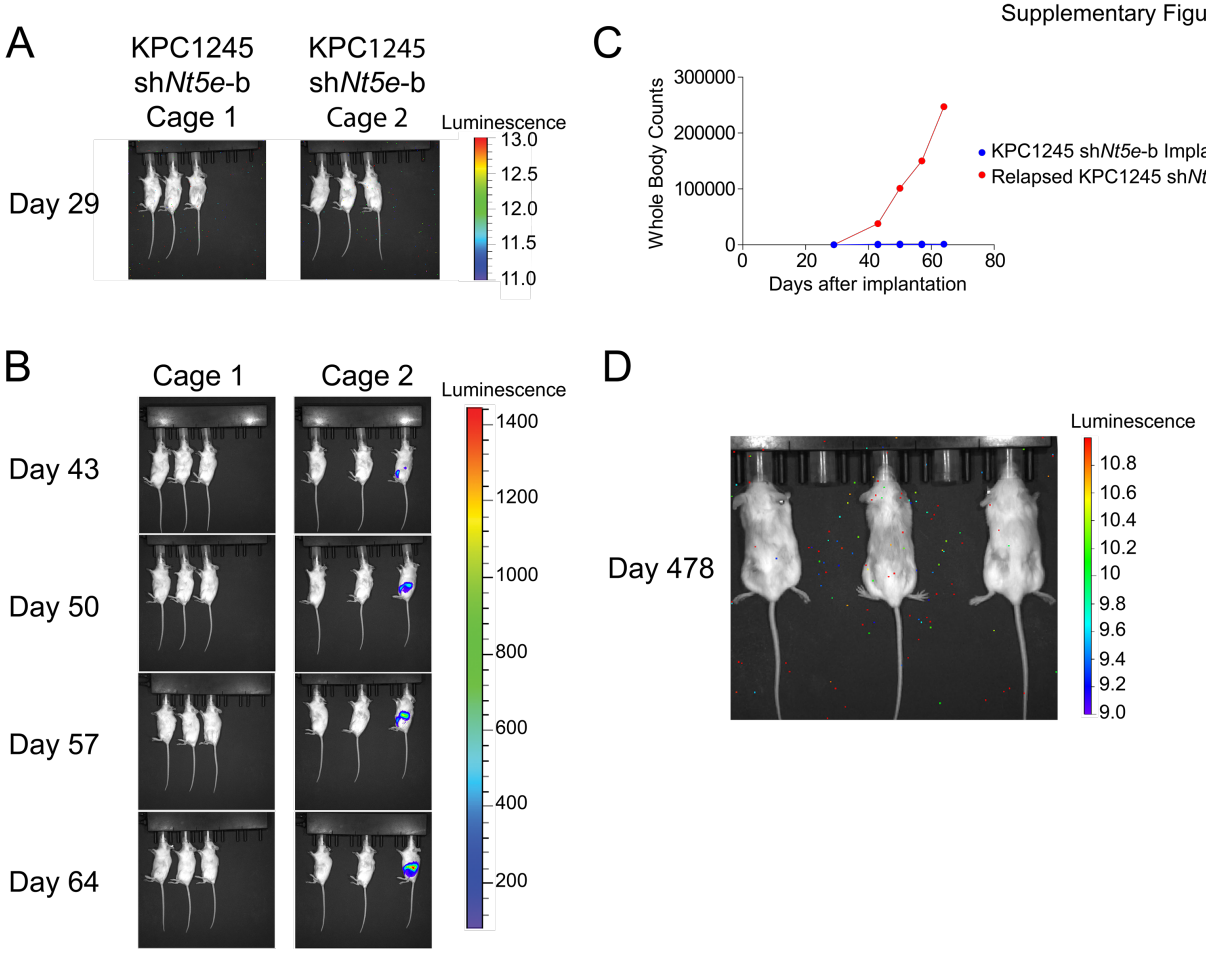

Supplementary Figure 2. Long term survival and relapse observed in CD73 knockdowns. B6(Cg)-*Tyr*$^{c\text{-}2J}$/J mice were orthotopically implanted with 5x10^3 luciferase positive KPC1245 *Nt5e* knockdown or control cells. Upon necropsy, control mice had tumors while little-to-no tumor was observed in sh*Nt5e*-a (n=10) and sh*Nt5e*-b (n=4). The remaining mice (n=6) were spared and monitored if they will develop a tumor. **A** Mice were injected with luciferin to detect any tumor, as it appeared negative in the necropsy. **B** Mice were observed weekly and found one mouse that developed a tumor. **C** Whole-body counts with the same area were measured for each mouse. The red line indicates the mouse that developed a tumor, while the blue lines are the other mice. The observation ended several weeks later; however, one more mouse developed a tumor and died on day 175. **D** 478 days later, cage 1 was examined for presence a luminescence signal after injecting luciferin.

Supplementary Figure 3

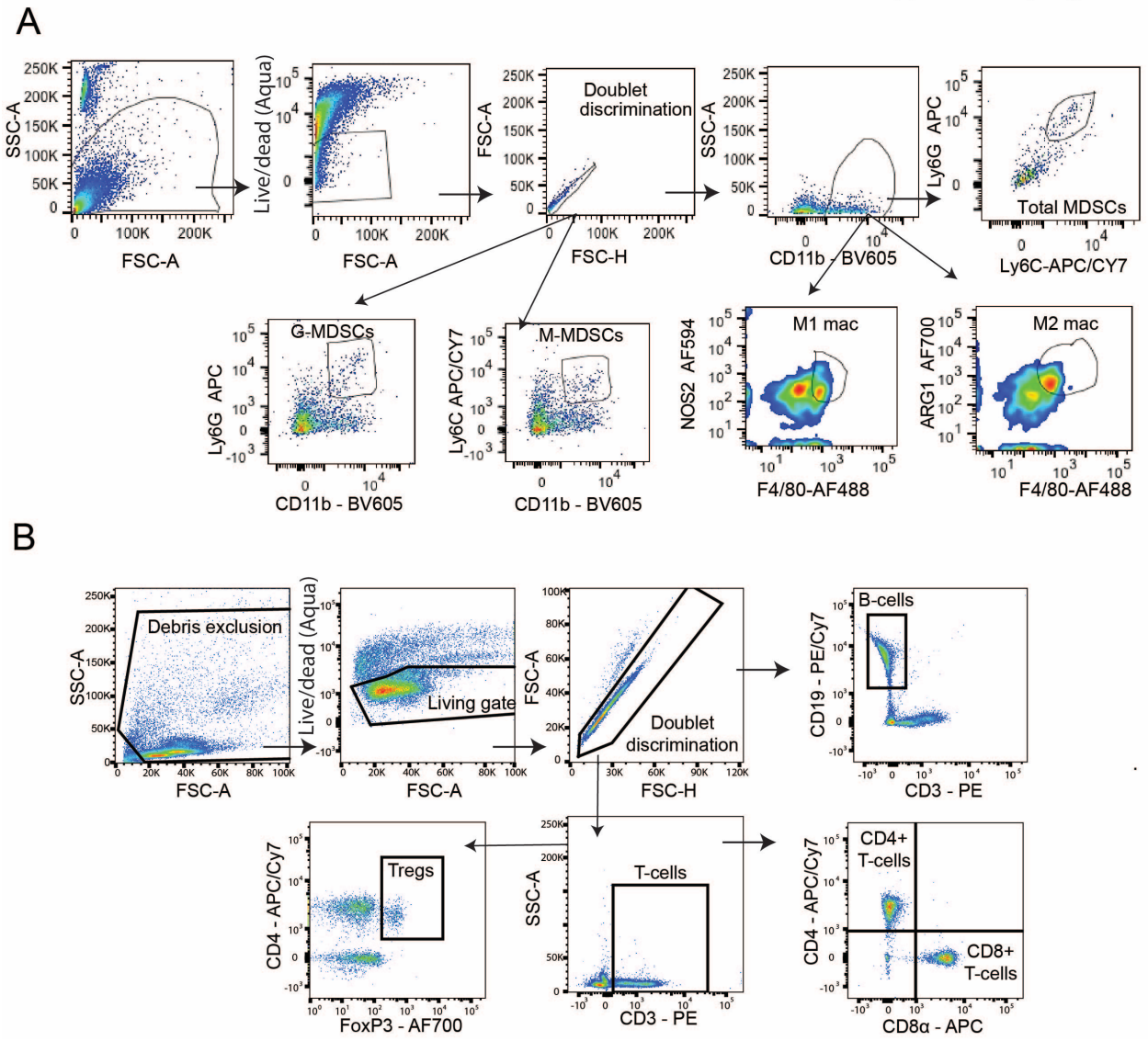

Supplementary Figure 3: Schematic representation of the gating strategy for immune cell profiling in tumor and blood from pancreatic tumor-bearing mice. A Schematic flow for analyzing G-MDSCs, M-MDSCs, M1-macrophages and M2-macrophages. **B** Schematic flow for analyzing T cells in blood and tumors.

Supplementary Figure 4

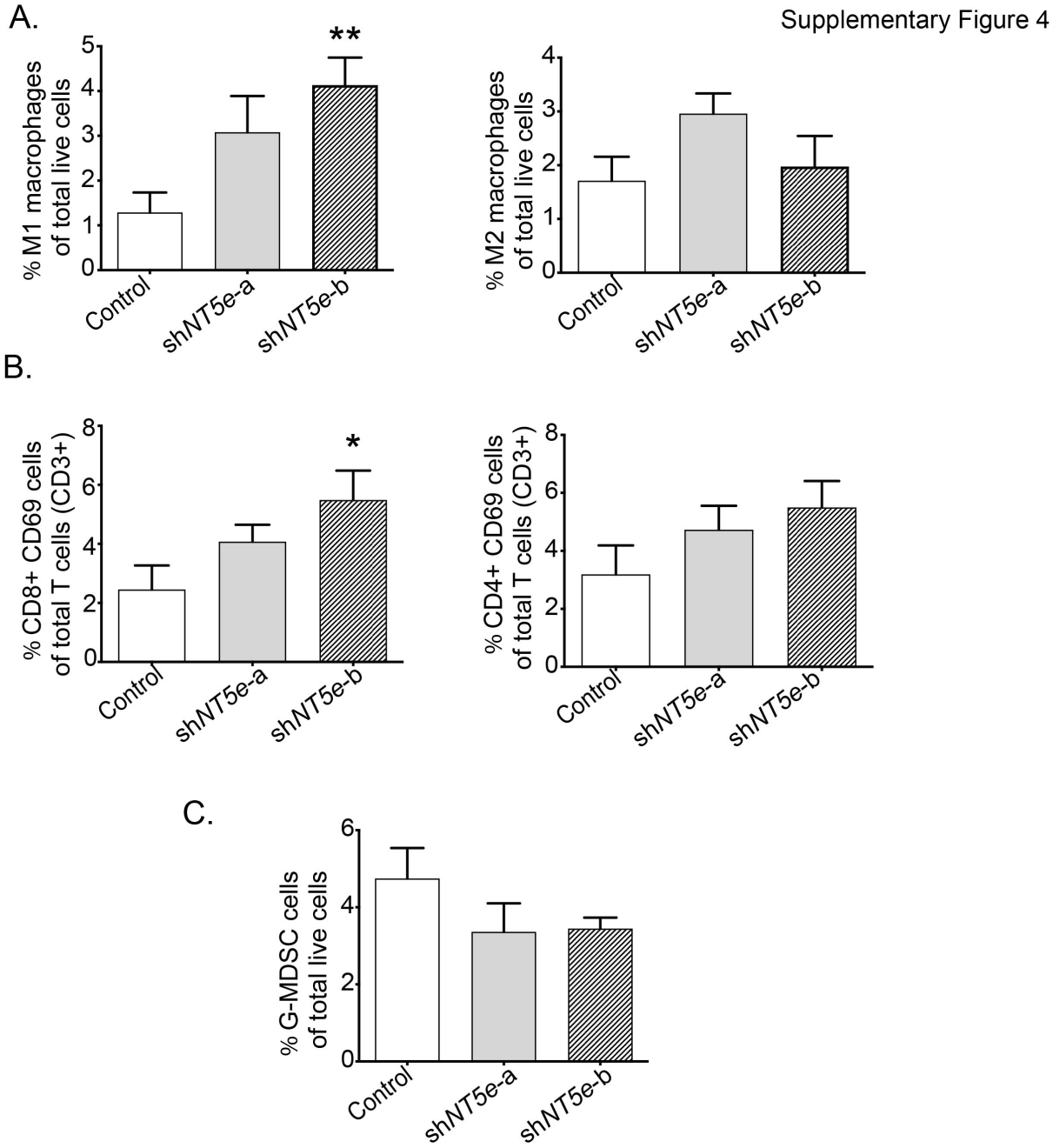

Supplementary Figure 4: ***Nt5e* knockdown tumors display increased proportion of M1 macrophages and attenuated levels of M-MDSCs**. B6(Cg)-*Tyr*$^{c\text{-}2J}$/J mouse pancreatic tumors from control and *Nt5e* knockdown tumor-bearing mice were harvested and processed for single-cell suspension and stained for surface and intracellular proteins. **A** Proportion of M1 (NOS2^{+} F4/80^{+} CD11b^{+}) macrophages and M2 (Arg1^{+} F4/80^{+} CD11b) macrophages in *Nt5e* knockdown tumor-bearing mice compared to controls. **B** Activated CD8 T cells (CD8^{+} CD69^{+}) and CD4 T cells (CD4^{+} CD69^{+}), respectively in *Nt5e* knockdown tumors. **C** G-MDSCs (Ly6G^{+} CD11b^{+}) in *Nt5e* knockdown tumors compared to control tumors [control (n=7), sh*Nt*5e-a (n=6), sh*Nt*5e-b (n=9)]. Bar charts were compared with a one-way ANOVA with Tukey's multiple comparison Test. Error bars depict the standard error of the mean. *P < 0.05, **P < 0.01.

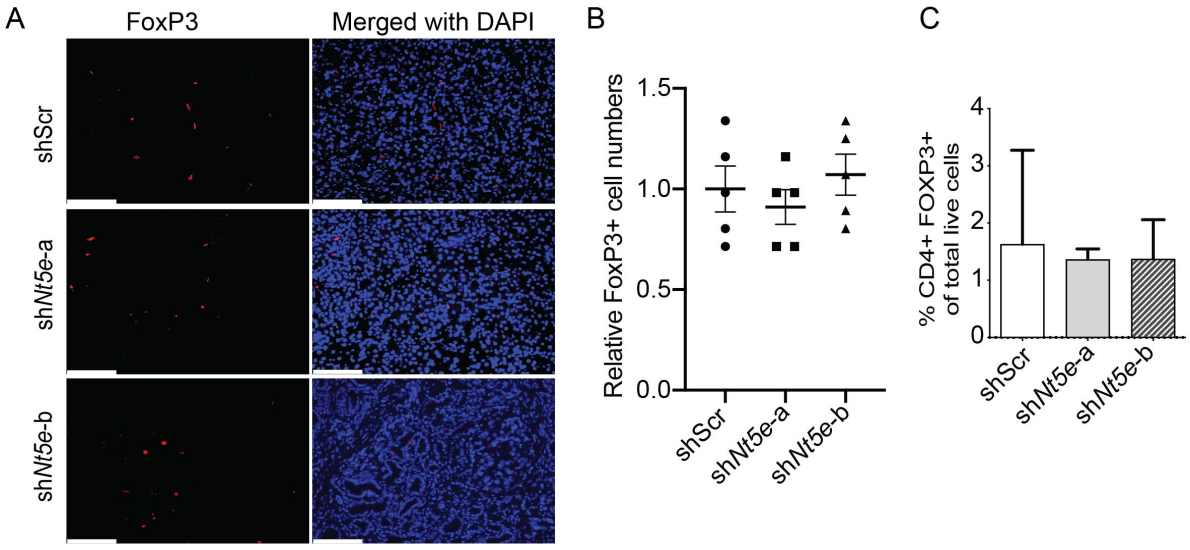

Supplementary Figure 5: FoxP3+ cell numbers in control and *Nt5e* knockdown tumors and circulation. A-B Representative immunofluorescence images (**A**) and quantitation of FoxP3 staining (**B**) in orthotopic tumors from B6(Cg)-*Tyr*$^{c\text{-}2J}$/J mice implanted with control and *Nt5e* knockdown KPC1245 cells. Scale bar: 123.4 μm. (**C**) Representative bar chart demonstrating circulating Treg population in B6(Cg)-*Tyr*$^{c\text{-}2J}$/J mice with control and *Nt5e* knockdown KPC1245 orthotopically implanted tumors [ShScr (n=7), shNt5e (n=8)]. Data was compared by one-way ANOVA with Tukey's multiple comparison test. Error bars depict the standard error of the mean.

Supplementary Figure 6

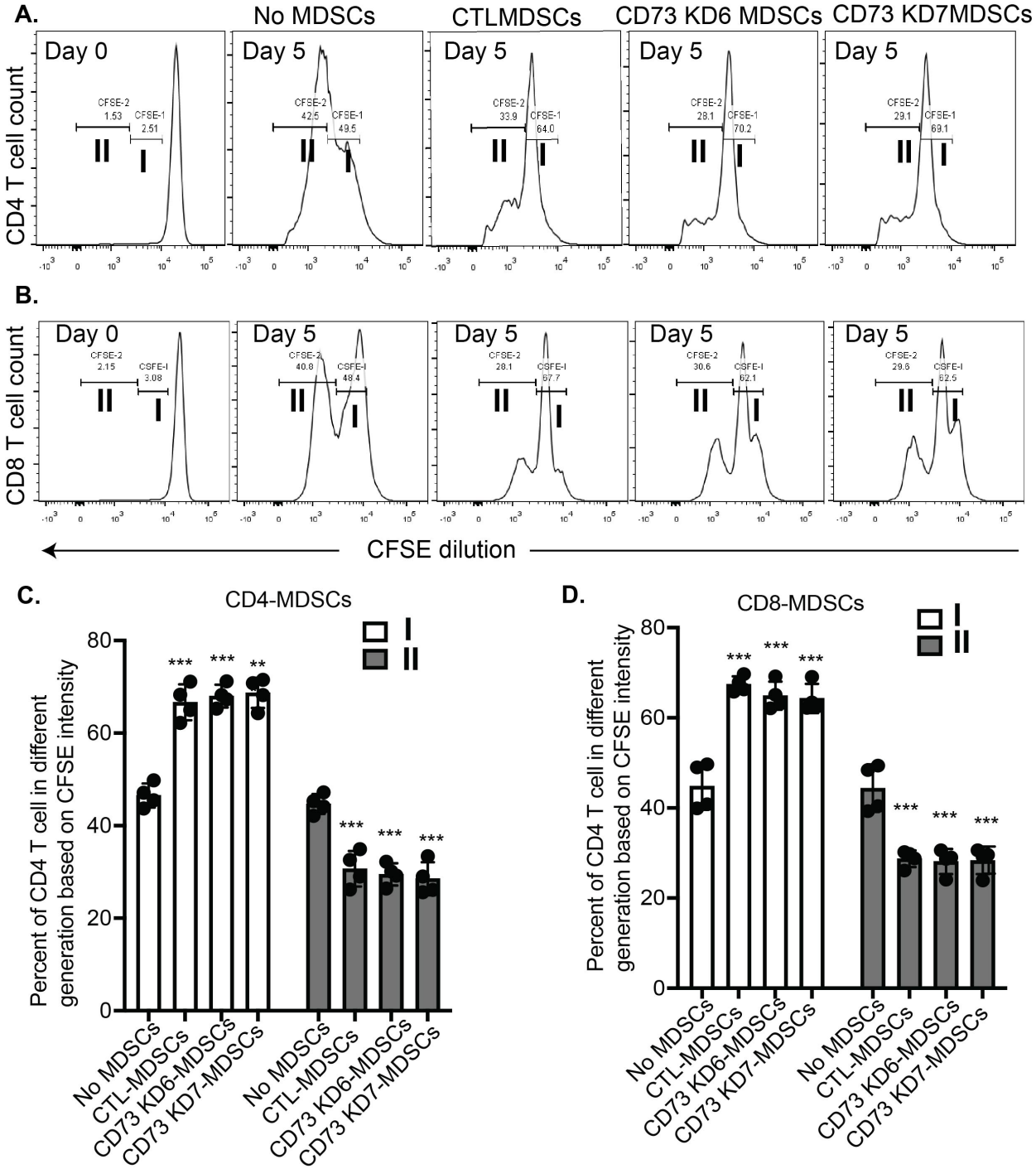

Supplementary Figure 6: CD8 T cell proliferation suppression by MDSCs from tumor-bearing mice. **A-B** Representative image depicts suppression of CD4 T cell (**A**) and CD8 T cell (**B**) proliferation by MDSCs derived from control and *Nt5e* knockdown tumor-bearing C57BL6/J mice. **C-D** Bar charts demonstrate the percentage of CFSE+ population in different generations (**I, II**) in CD4 T cells (**C**) and CD8 T cells (**D**) post co-

culture with MDSCs. MDSCs were enriched from splenocytes from control or *Nt5e* knockdown C57BL6/J tumor-bearing mice and co-cultured for 6 days with CFSE-labelled and previously stimulated (anti-CD3+anti-CD28) naive CD8 T cells, in a 2:1 ratio in the presence of mouse recombinant IL-2 (20ng/ml). Post incubation, cells were labelled with anti-CD4 and anti-CD8 antibodies and analyzed by a flow cytometer. Error bars depict the standard error of the mean. Data was analyzed by ANOVA with Tukey's multiple comparison test, *** $P < 0.001$.

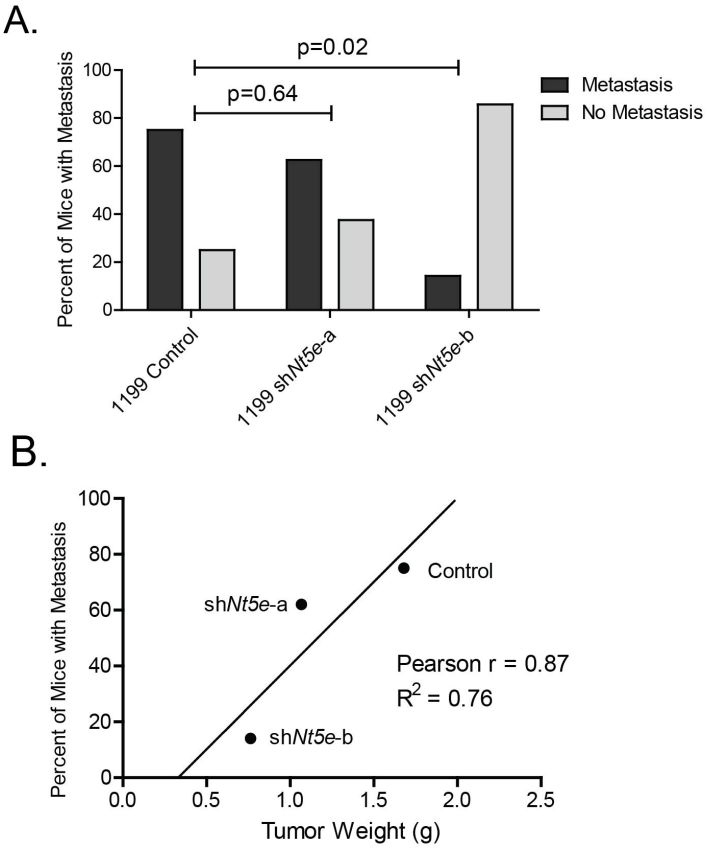

Supplementary Figure 7: CD73 knockdown decreases metastasis in sh*Nt5e*-b tumor-bearing mice. A Bar chart displaying the percentage of control and *Nt5e* knockdown tumor-bearing athymic nude mice exhibiting metastasis with Fisher's exact test for significance. **B** Scatter plot showing a positive association between the tumor weight and the incidence of metastasis. Data was fit with a linear regression and the Pearson's r is shown, but p value is not significant. Athymic nude mice were implanted with KPC1199 control (n=7), sh*Nt5e*-a (n=6), and sh*Nt5e*-b (n=9) cell lines and are the mice from Fig. 4A-D.

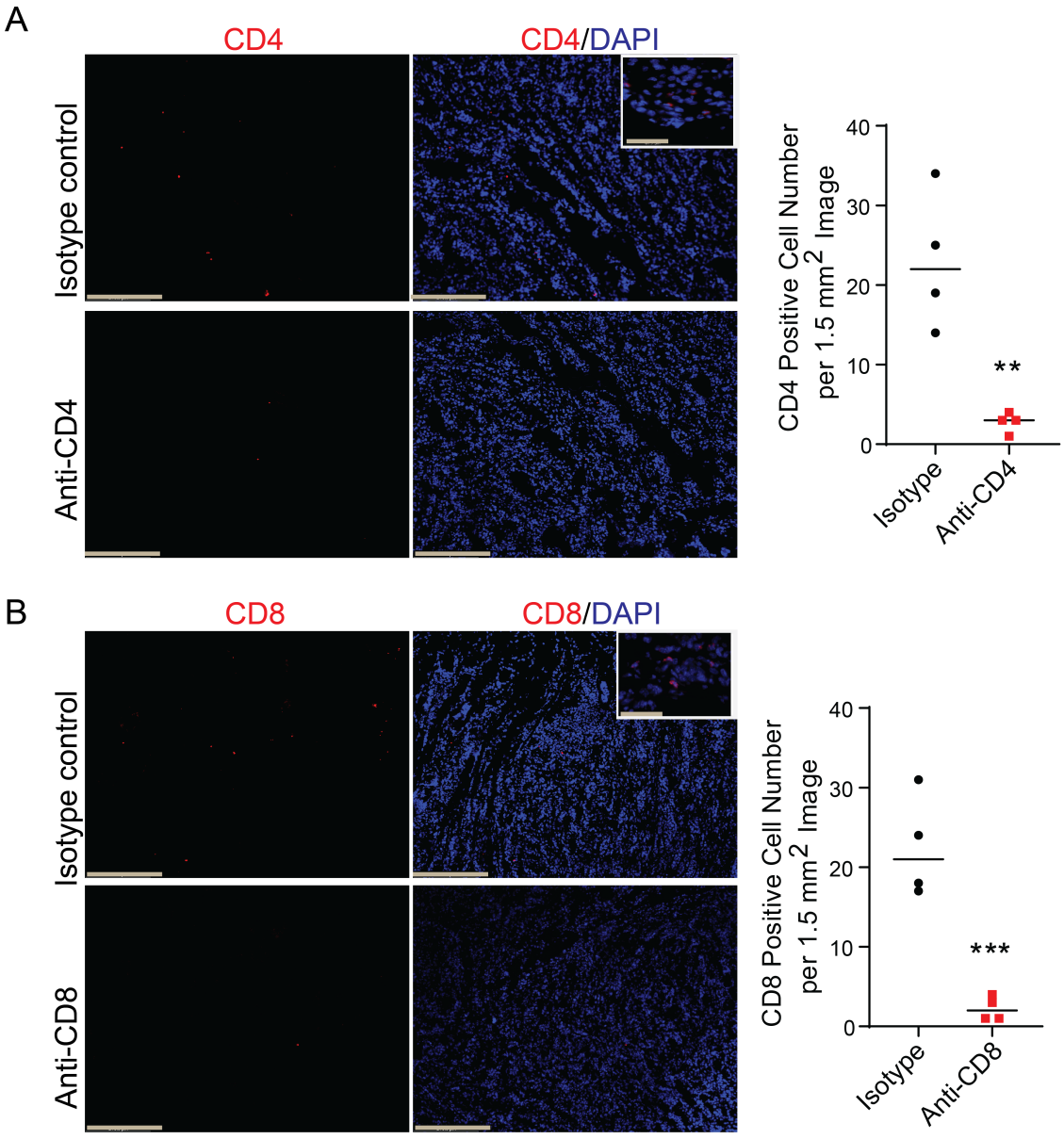

Supplementary Figure. 8: CD8 and CD4 depletion in tumor-bearing mice. **A-B** Immunohistochemistry images display CD4 (**A**) and CD8 T cell (**B**) staining in tumors from the isotype control or anti-CD8 and anti-CD4 antibody-treated B6(Cg)-*Tyr*$^{c\text{-}2J}$/J mice. Corresponding strip charts demonstrate the frequency of each T cell subtype in different treatment cohorts. Scale bar is 250μm in the 10x images and 56μm in the insets. Data was compared by unpaired t-test. *P < 0.05, **P < 0.01, ***P < 0.001.

Supplementary Figure 9

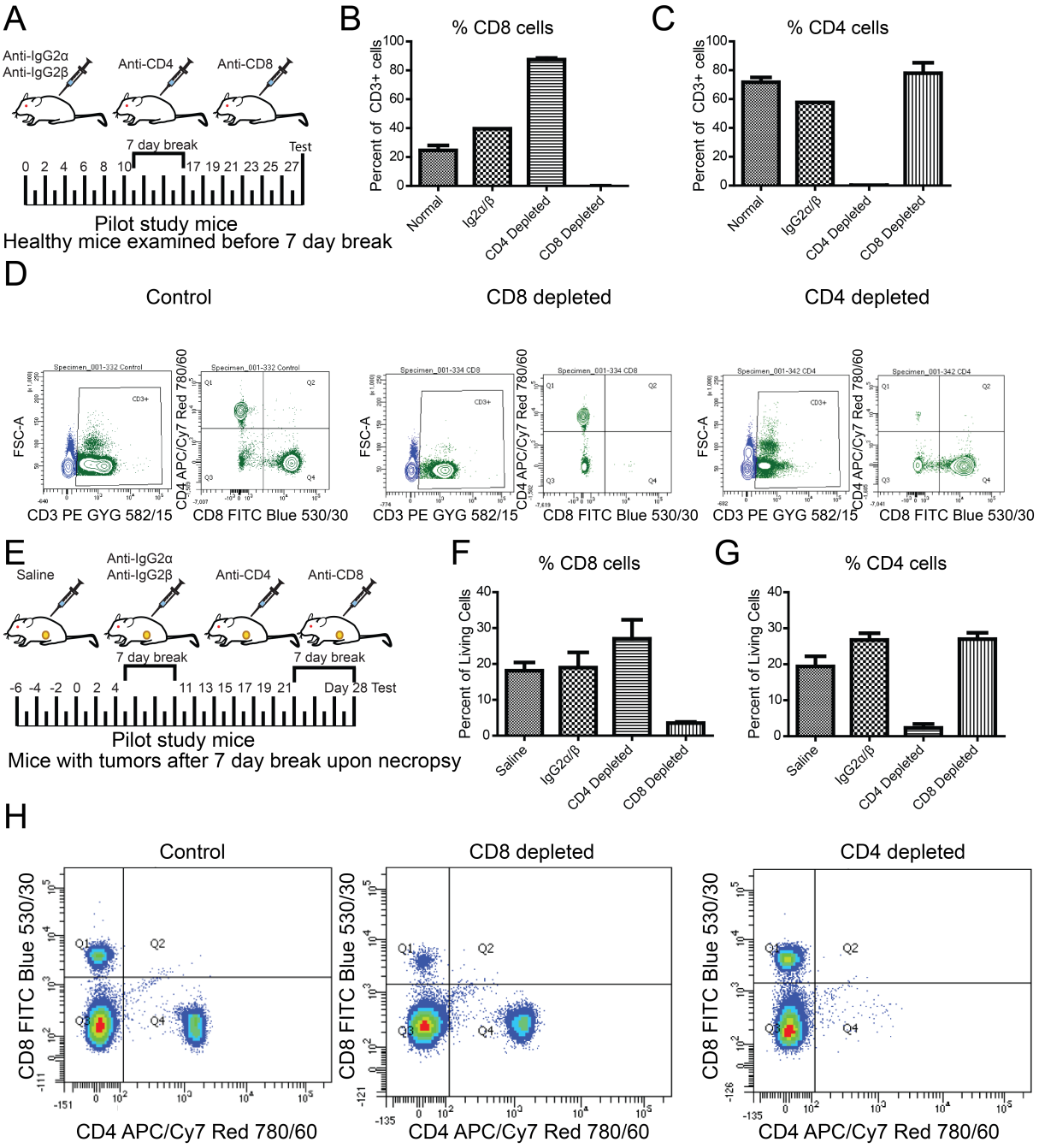

Supplementary Figure 9: Immune depletion validation. Pilot experiments were carried out to verify CD4 and CD8α depletion. **A** Layout of the injection schedule and experimental cohorts, which also included healthy age-matched mice as a control (normal). **B-C** Peripheral blood was collected through submandibular bleeding and gated for size, viability, and CD3ε$^+$ before gating for CD8α$^+$ (**B**) and CD4$^+$ (**C**). **D** Representative gating after gating for size and viability. **E** Depletion strategy of mice implanted with 5x10^3 KPC1245 cells to examine depletion. **F-G** Submandibular peripheral blood was gated for size, viability, and CD3ε$^+$ before gating for CD8α$^+$ (**F**) and CD4$^+$ (**G**). **H** Representative

gating after gating for size, viability, and CD3ε^{+} cells. Error bars depict the standard error of the mean.

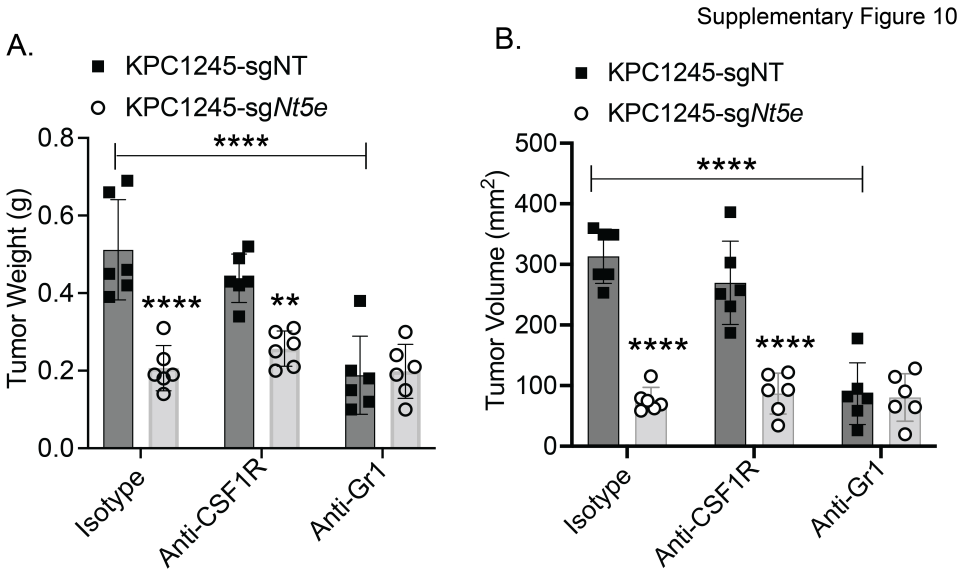

Supplementary Figure 10: MDSC, but not macrophage, depletion attenuates tumor burden in KPC1245-sgNT control tumor bearing mice. Bar charts represent tumor weight (**A**) and volume (**B**) in different treatment cohorts of orthotopic KPC1245-sgNT or *Nt5e* knockout (KPC1245-sgCD73) tumor-bearing B6(Cg)-*Tyr*$^{c\text{-}2J}$/J mice. Mice were treated with anti-CSF1R (200ug, i.p, 3 times per week, starting 2 days prior tumor implantation) and anti-Gr-1 (200ug, i.p, every two days starting two days before implantation) for depletion of macrophage and MDSCs, respectively. Control mice were treated with isotype control Rat IgG2b and Rat IgG2a antibodies, following the dose and schedule corresponding to the anti-CSF1R and anti-Gr-1 antibodies. Data was compared by two-way ANOVA with Tukey's multiple comparison test. Error bars depict the standard error of the mean, *P < 0.05, **P < 0.01, ****P< 0.0001.

Supplementary Figure 11

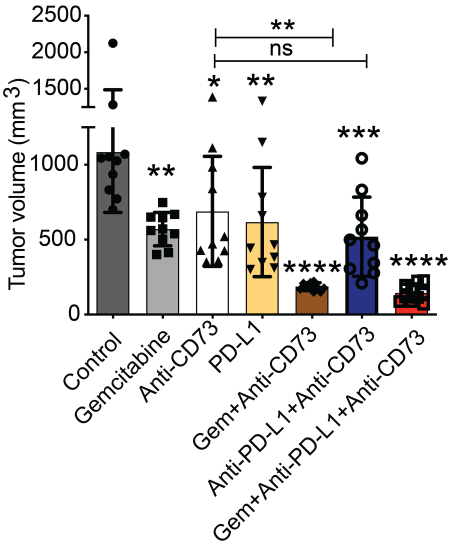

Supplementary Figure. 11: Anti-CD73 and gemcitabine combination demonstrates better therapeutic efficacy than anti-CD73 or immune checkpoint blocker (anti-PD-L1) treatments. Bar chart demonstrates tumor volume at day 28 post orthotopic KPC1245 tumor cell implantation in B6(Cg)-*Tyr*$^{c\text{-}2J}$/J male mice. Mice were treated with anti-CD73 (100ug, i.p, three times per week), anti-PD-L1 (200ug, i.p., twice were week) and gemcitabine (50mg/kg, i.p., twice per week in 100µL saline). Data for each set was compared to the control, or as indicated, by one-way ANOVA with Tukey's multiple comparison test. Error bars depict the standard error of the mean, *P < 0.05, **P < 0.01, ***P < 0.001, ****P< 0.0001.

Supplementary Tables:

Supplementary Table 1. Enzyme survival p-values from mRNA Z-score cohorts. Pancreatic cancer patients from The Cancer Genome Atlas (TCGA) were split into cohorts based on if the mRNA was lower, similar, or higher than normal mRNA based on if it was more than two standard deviations below (low), above (high), or within (normal) two standard deviations from the normal adjacent tissue mRNA expression. All cohorts were analyzed pairwise or together in the all category. P-values represent the significance of a Mantel-Haenszel log-rank test.

Supplementary Table 2. Enzyme survival p-values from mRNA interquartile range cohorts. Pancreatic cancer patients from The Cancer Genome Atlas (TCGA) were split into cohorts based on if the mRNA was in the <25% (low), 25%-75% (normal), or >75% (high) interquartile range. P-values represent the significance of a Mantel-Haenszel log-rank test. All cohorts were analyzed together in the all category.

Supplementary Table 3. Survival p-values of all available genes from mRNA interquartile range cohorts. Pancreatic cancer patients from The Cancer Genome Atlas (TCGA) were split into cohorts based on if the mRNA was in the <25% (low), 25%-75% (normal), or >75% (high) interquartile range. P-values represent the significance from a Mantel-Haenszel log-rank test. All cohorts were analyzed pairwise or together in the all category. P-values represent the significance of a Mantel-Haenszel log-rank test.